

IMAGE TAG COMPLETION BY LOW-RANK FACTORIZATION WITH DUAL RECONSTRUCTION STRUCTURE PRESERVED

Xue Li ^a, Yu-Jin Zhang ^a, Bin Shen ^b, Bao-Di Liu ^c

^a Electronic Engineering, Tsinghua University, Beijing, 100084, China

^b Computer Science, Purdue University, West Lafayette, IN 47907, USA

^c Information and Control Engineering, China University of Petroleum, Qingdao, 266580, China
xue-li11@mails.tainghua.edu.cn, zhang-yj@mail.tsinghua.edu.cn

ABSTRACT

A novel tag completion algorithm is proposed in this paper, which is designed with the following features: 1) *Low-rank and error sparsity*: the incomplete initial tagging matrix D is decomposed into the complete tagging matrix A and a sparse error matrix E . However, instead of minimizing its nuclear norm, A is further factorized into a basis matrix U and a sparse coefficient matrix V , *i.e.* $D = UV + E$. This low-rank formulation encapsulating sparse coding enables our algorithm to recover latent structures from noisy initial data and avoid performing too much denoising; 2) *Local reconstruction structure consistency*: to steer the completion of D , the local linear reconstruction structures in feature space and tag space are obtained and preserved by U and V respectively. Such a scheme could alleviate the negative effect of distances measured by low-level features and incomplete tags. Thus, we can seek a balance between exploiting as much information and not being misled to suboptimal performance. Experiments conducted on Corel5k dataset and the newly issued Flickr30Concepts dataset demonstrate the effectiveness and efficiency of the proposed method.

Index Terms— Tag completion, Image annotation, Low-rank, Error sparsity, LLE

1. INTRODUCTION

With digital imaging gains its popularity in recent decades, the demand for effective and efficient automatic image annotation (AIA) methods is highlighted by both content based image retrieval (CBIR) [1–3] and tag based image retrieval (TBIR). Nevertheless, performance of most existing AIA [4–6] methods degrades dramatically when initial tags are noisy or incomplete, thus how to perform accurate tag completion has become a hot issue that needs to be addressed.

Among the various proposed methods [7–13] for tag completion, the pursuit of maintaining content consistency and tag relationship has always been a key component in nearly every algorithm, though in different formulations. G. Zhu *et al.* [7] defined two similarity matrix in both feature space and tag space, and violations of such similarity resulted from the completed matrix are minimized. Similarly, in [10], X.Liu *et al.* promoted feature-label harmoniousness and punished interlabel discrepancy. The recently proposed TMC method [8] aimed at preserving correlation structures for images and

tags in the completed matrix, and the LSR method [9] performed linear sparse reconstruction for each image and each tag, respectively. According to their reported performance, LSR is better than existing methods, especially the ones defining similarity based on distance in feature space or initial tags, since similar features do not necessarily guarantee related tags due to the semantic gap, and distances measured by incomplete tags are unreliable. Therefore, the usage of such distances may introduce risks and mislead the completion process. On the other hand, analogous to Local Linear Embedding (LLE) [14], the LSR method restricts the related images or tags to be within the same subspace and preserves local geometry, which means the noisy distances are not involved in this framework, thus the influences of semantic gap and incomplete tags get alleviated.

Another debated issue involves the low-rank constraint. As pointed out in [7], low-rank constraint is natural since the semantic space spanned by tags is low-rank, whereas [9] indicates that the low-rank constraint may be more suitable for denoising rather than completion, and it is difficult to control the degree of denoising. However, methods that do not utilize low-rank property strongly rely on initial tags, since they lack the ability to recover latent structures with noisy incomplete data.

Motivated by the foregoing analysis, our formulation is designed with the following features:

- **Low-rank and error sparsity.** The initial tagging matrix D is decomposed into a sparse error matrix E and a factorization of a basis matrix U and a sparse coefficient matrix V , *i.e.* $D = UV + E$. This low-rank formulation encapsulating sparse coding [15–19] has the ability to recover the latent complete matrix from noisy data and at the same time avoid performing too much denoising, which is a main problem of [7].
- **Local reconstruction structure consistency.** As discussed above, using distances measured by low-level features and incomplete tags may introduce risks and mislead the completion process. Therefore, similar to [9], the proposed method also rests on the LLE assumption and attempts to preserve the local linear reconstruction structures in *both* the feature space and tag space.

The main contribution of the proposed formulation lies in the combination and extension of low-rank property and local reconstruction structure consistency. For the former, despite its ability to recover low-rank structures from noisy data, minimizing nuclear norm is more suitable for the reconstruction of dense matrix, thus it may tend to perform filtering rather than completion, and the recovered tags may not be accurate enough, especially when A itself is

This work was supported by National Nature Science Foundation (NNSF: 61171118) and Specialized Research Fund for the Doctoral Program of Higher Education (SRFDP-20110002110057).

sparse. In order to fix this, the proposed method uses sparse coding for the reconstruction of the low-rank final matrix A , which can then seek a balance between accurate reconstruction and robustness towards initial noisy data; For the latter, as an extension of [9], the local geometry structures are preserved in the compressed low-dimensional feature space and tag space, which is more suitable for our low-rank framework and to steer the generation of U and V . Note that the local geometry structures in the original space is guaranteed to be preserved in this way.

The rest of this paper is organized as follows. The novel formulation for tag completion is elaborated in Section 2, followed by detailed optimization methods in Section 3. Experimental results on two datasets are presented in Section 4, and Section 5 concludes this paper.

2. TAG COMPLETION BY LOW-RANK FACTORIZATION WITH DUAL LOCAL RECONSTRUCTION STRUCTURE PRESERVED

Denote the initial user-provided tagging matrix as $D_{N \times M}$, with M and N specifying the number of tags and images, respectively. Entries in D have binary values, that is,

$$D_{ij} = \begin{cases} 1, & \text{in case image } i \text{ is associated with label } j; \\ 0, & \text{otherwise.} \end{cases} \quad (1)$$

Our goal is to recover the latent complete tagging matrix A . Following the framework in [7], D is also decomposed into the complete matrix A and a sparse error matrix E ; Since A is believed to be of low-rank, then it can be further factorized as $A = UV$. Thus,

$$D = UV + E \quad (2)$$

where $U_{N \times K}$ and $V_{K \times M}$ are the basis and sparse coefficient matrix, respectively.

As mentioned in Section 1, low-rank is achieved using a sparse coding scheme, and preserve local reconstruction structures in the compressed low-dimensional feature space and tag space. Details of the proposed method is presented in the following subsections.

2.1. Low Rank and Error Sparsity

In order to make our method robust to initial noisy labels, the proposed method follows the framework developed in [7] and adopts the low-rank constraint. However, in order to fix the problem pointed out by [9], the complete tagging matrix A is factorized as $A = UV$, instead of minimizing its nuclear norm. Here V can be viewed as tag representation in new low-dimensional tag space, and U as image representation in new low-dimensional image space. Thus, our basic objective function can be written as follows:

$$\begin{aligned} & \min_{U,V,E} \left\{ \|D - E - UV\|_F^2 + 2\eta \|V\|_1 + \beta \|E\|_1 \right\} \\ \text{s.t.} \quad & \|U_{\bullet k}\|_2 = 1, \forall k \in 1, 2, \dots, K \end{aligned} \quad (3)$$

Note that Eq.(3) can be interpreted as sparse coding, with $U_{N \times K}$ being the basis matrix and $V_{K \times M}$ the sparse coefficient matrix. Such a scheme can achieve fine-grained approximation and control the degree of denoising, which makes it more suitable for completion tasks. The error matrix E also has the ability to prevent it from completely reconstructing D .

2.2. Local Reconstruction Structure in Feature Space

Denote $X_{N \times L}$ as the feature matrix in the original space, each row of X is a feature vector of an image. In the new low-dimensional space, each row of U is a compressed representation of an image. Similar to the idea of LLE, the local geometry structure is believed to be important and should be preserved while compressing the representation. Thus, first the original data X is explored for the structure information, which is encoded in matrix S :

$$\begin{aligned} S^* &= \arg \min_S \left\{ \|X - SX\|_F^2 + \alpha \|S\|_1 \right\} \\ \text{s.t.} \quad & S_{nn} = 0, \forall n \in 1, 2, \dots, N \end{aligned} \quad (4)$$

where $S_{N \times N}$ is the local linear reconstruction coefficient matrix in feature space.

The j -th row of S contains corresponding weights that can be used to reconstruct the features of the j -th image using that of other images.

Eq.(4) can be efficiently solved using the feature-sign method [20].

Next, assume the tags of the j -th image can be equally reconstructed by the tags of other images, thus $A \sim SA$. The local linear reconstruction structure specified by S should be robust to the sparse coding procedure in Eq.(3), which means this reconstruction structure should applies to U as well, *i.e.* $U \sim SU$. Therefore, the objective function can be rewritten as:

$$\begin{aligned} & \min_{U,V,E} \left\{ \|D - E - UV\|_F^2 + \gamma \|U - SU\|_F^2 \right. \\ & \quad \left. + 2\eta \|V\|_1 + \beta \|E\|_1 \right\} \\ \text{s.t.} \quad & \|U_{\bullet k}\|_2 = 1, \forall k \in 1, 2, \dots, K \end{aligned} \quad (5)$$

2.3. Local Reconstruction Structure in Tag Space

Similarly, each column of V can be viewed as compressed feature of a tag, and the local reconstruction structure in the original tag space should be preserved. So, the structure information, encoded in T , is explored first in the original data D :

$$\begin{aligned} T^* &= \arg \min_T \left\{ \|D - DT\|_F^2 + \mu \|T\|_1 \right\} \\ \text{s.t.} \quad & T_{mm} = 0, \forall m \in 1, 2, \dots, M \end{aligned} \quad (6)$$

where $T_{M \times M}$ is the local linear reconstruction coefficient matrix in tag space.

The i -th column of T contains corresponding weights that can be used to reconstruct the distribution of the i -th tag using that of other tags.

Then the reconstruction relationship specified by T should also applies to V . Therefore, our final objective function is as follows:

$$\begin{aligned} & \min_{U,V,E} \left\{ \|D - E - UV\|_F^2 + \gamma \|U - SU\|_F^2 + \right. \\ & \quad \left. \lambda \|V - VT\|_F^2 + 2\eta \|V\|_1 + \beta \|E\|_1 \right\} \\ \text{s.t.} \quad & \|U_{\bullet k}\|_2 = 1, \forall k \in 1, 2, \dots, K \end{aligned} \quad (7)$$

Eq.(6) can be solved analogous to Eq.(4).

3. OPTIMIZATION

In this section, we focus on solving the minimization of the proposed objective function in Eq.(7). Although it is not jointly convex in all three variables, it is separately convex in U , V and E with remaining variables fixed. Thus, Eq.(7) can be solved by decoupling it into three subproblems and conducting optimization separately.

3.1. Optimizing Coefficient V

Here the method in [16] is used. Define $\tilde{D} = D - E$, $H = \lambda(T - I)(T - I)^T$, when U and E are kept fixed, Eq.(7) reduces to:

$$\begin{aligned} f(V) &= \|\tilde{D} - UV\|_F^2 + \lambda\|V - VT\|_F^2 + 2\eta\|V\|_1 \\ &= \text{tr}\{\tilde{D}^T\tilde{D} - 2V\tilde{D}^T U + VV^T U^T U\} \\ &\quad + \text{tr}\{VHV^T\} + 2\eta\|V\|_1 \end{aligned} \quad (8)$$

Ignoring the constant term $\text{tr}\{\tilde{D}^T\tilde{D}\}$, the objective function of V_{km} reduces to

$$\begin{aligned} f(V_{km}) &= 2V_{km} \left[\sum_{\substack{l=1 \\ l \neq k}}^K V_{lm}(U^T U)_{lk} + \sum_{\substack{r=1 \\ r \neq m}}^M H_{mr}V_{kr} - (\tilde{D}^T U)_{mk} \right] \\ &\quad + V_{km}^2 [(U^T U)_{kk} + H_{mm}] + 2\eta|V_{km}|. \end{aligned} \quad (9)$$

Note that Eq.(9) is a piece-wise parabolic function that opens up, which is convex and easy to obtain the optimal point

$$V_{km} = \frac{\max\{P_{km}, \eta\} + \min\{P_{km}, -\eta\}}{(U^T U)_{kk} + H_{mm}} \quad (10)$$

where

$$P_{km} = (\tilde{D}^T U)_{mk} - \sum_{\substack{l=1 \\ l \neq k}}^K V_{lm}(U^T U)_{lk} - \sum_{\substack{r=1 \\ r \neq m}}^M H_{mr}V_{kr}$$

3.2. Optimizing Basis U

Optimization of U can be conducted by alternating between a procedure similar to V and Euclidean projection.

Define $G = \gamma(S - I)^T(S - I)$, when V and E are fixed, U can be solved analogous to V , the only modification is to remove the L_1 regularizer:

$$U_{nk} = \frac{Q_{nk}}{(VV^T)_{kk} + G_{nn}} \quad (11)$$

where

$$Q_{nk} = (V\tilde{D}^T)_{kn} - \sum_{\substack{l=1 \\ l \neq k}}^K (VV^T)_{kl}U_{nl} - \sum_{\substack{r=1 \\ r \neq n}}^N U_{rk}G_{rn}$$

Then, Euclidean projection is performed to ensure the L_2 norm of each column in U is less than 1. Note this is coordinate descend approach and the projection is conducted after each coordinate is updated if the L_2 norm of the updated column of U is greater than 1. Thus, both convergence and the decrease in objective function are guaranteed. This constraint of $\|U_{\bullet k}\| = 1$ is relaxed to $\|U_{\bullet k}\| \leq 1$, since the relaxation will result in a convex optimization problem while keeping the global optimum unchanged. *i.e.* the optimal U will always satisfy $\|U_{\bullet k}\| = 1$ even if our explicit constraint is $\|U_{\bullet k}\| \leq 1$.

3.3. Optimizing Sparse Error E

Finally, when U and V are fixed, obtaining E reduces to solving the following sparse coding problem:

$$E^* = \arg \min_E \left\{ \|D - UV - E\|_F^2 + \beta\|E\|_1 \right\}, \quad (12)$$

which can be solved similar to S and T .

3.4. Implementation Issues

A kNN (k Nearest Neighbors) strategy is adopted when calculating matrix S and T , where $k = 200$ (same to [9]), in order to make it faster. For the number of basis, $K = 100$ is used in Corel5k dataset, and $K = 500$ for the much larger Flickr30Concepts dataset.

Meanwhile, similar to [7], D is re-initialized as $D = (SD + DT)/2$ before fed to the completion process.

Also, for the Flickr30Concepts dataset, tags are treated as features when obtaining S . Tags are not used as features in Corel5k dataset, since the remaining tags of images in Corel5k are very sparse (less than 5), thus using tags as features would cause performance deterioration.

4. EXPERIMENTS

In this section, our experimental setup is first outlined, followed by the analysis of some parameters. Finally, the performance of the proposed fomulation is evaluated and compared with prior methods.

4.1. Datasets and Measurement

To facilitate comparison between our method and previous ones, the same datasets and features as in [9] are used. Two datasets are used: the well-established benchmark dataset Corel5k and the real-world Flickr30Concepts. Statistics of both datasets are given in Table 1.

For Corel5k dataset, 40% of tags are randomly deleted which ensures that each image has at least one tag removed and one tag remained. The 1000-dimensional SIFT BoW feature is downloaded from <http://lear.inrialpes.fr/people/guillaumin/data.php>. Random deletion is performed 8 times and averaged performance is reported. Furthermore, a validation set containing 491 images is extracted randomly to perform parameter tuning.

For Flickr30Concepts dataset [9], the data provided by the authors are used, including the ground truth and the initial tagging matrix, along with two types of features: the 1000-dimensional SIFT BoW feature and the composite features consisting of a set of 10 kinds of basic features¹.

Also, the same test method as [9] is used, as with the same measurements: *average precision@N* (*i.e.* AP@N), *average recall@N* (*i.e.* AR@N) and *coverage@N* (*i.e.* C@N). Evaluations are only conducted for the test set, and extract neighbors only in the training set, for a fair comparison.

4.2. Parameter Settings

Altogether 6 parameters are involved in the proposed method, hence it is necessary to tune each parameter in order to achieve better performance and analyze their respective influence to the completion process.

¹The features include: Color Correlogram, Color Layout, CEDD, Edge Histogram, FCTH, JCD, Jpeg Coefficient Histogram, RGB Color Histogram, Scalable Color, SURF with Bag-of-Words model.

Table 1. Statistics of Core5k and Flickr30Concepts. Counts of tags are given in format of "mean/maximum".

	Core5k	Flickr30Concepts
Vocabulary Size	260	2,513
Nr. of Images	4,918	27,838
Tags per Image	3.4/5	8.3/70
Del. Tags per Image	1.4 (40%)	3.3 (40%)
Test Set	492	2,807

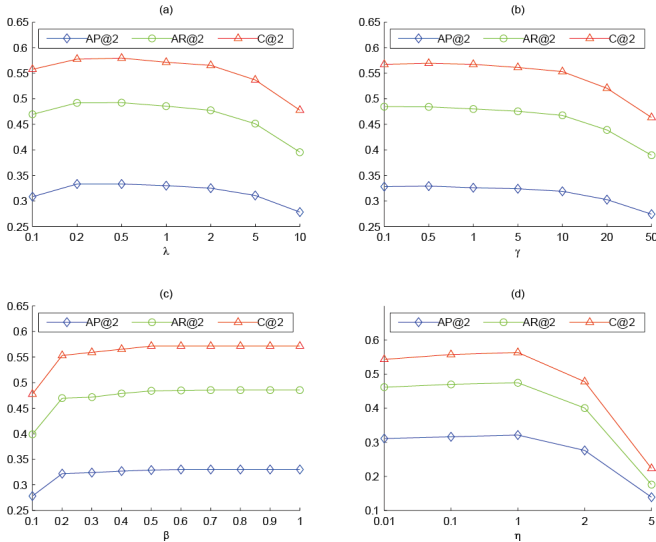


Fig. 1. Influences of λ , γ , β and η on validate set of Core5k.

The control variable method is adopted, which means modifying only one parameter at a time and keeping others unchanged. The results are shown in Fig.1. Since α and μ have little influence, so a large number (here 1) is used to make the feature-sign method faster.

As illustrated in Fig.1, the value of γ should not be too large, since a larger γ means a higher degree of confidence on the assumption that $SA \sim A$, whereas this maybe questionable due to the semantic gap. Similarly, performance also degraded as λ gets larger, since T is obtained from incomplete initial tags. A smaller β means a denser E , thus, as β vanishes, it would be difficult to achieve fine-grained reconstruction of D , so the completed tags may be inaccurate; On the other hand, if E gets too sparse, its ability to control the completion process would be weakened. Here too large values are not used since the feature-sign method would return all-zero matrix when β gets too large. For η , as it approaches 0, the L_1 regularizer seems disabled; as it gets larger, V maybe too sparse and the reconstruction error would get large. The final values adopted in our experiments are $\lambda = 0.5$, $\gamma = 1$, $\beta = 0.7$, $\eta = 1$.

4.3. Tag Completion Results

To demonstrate the effectiveness of our method, its performance is compared with state-of-the-art annotation methods (JEC [4] and TagProp [5]) and several newly proposed tag completion algorithms, namely TMC, DLC and LSR. Note that JEC and TagProp are designed for multi-features, while TMC and DLC are more suitable for SIFT BoW feature, whereas the LSR method, along with the proposed one, can handle both multi-features and SIFT BoW feature.

Table 2. Experimental results on Core5k and Flickr30Concepts with only SIFT BoW feature.

	Core5k ($N = 2$)			Flickr30Concepts ($N = 4$)		
	AP	AR	C	AP	AR	C
TMC	0.23	0.33	0.40	0.19	0.21	0.37
DLC	0.09	0.13	0.18	0.07	0.09	0.23
LSR	0.28	0.42	0.50	0.30	0.36	0.60
Ours	0.32	0.49	0.57	0.32	0.39	0.64

Table 3. Experimental results on Flickr30Concepts with 10 types of features.

	Flickr30Concepts ($N = 4$)		
	AP	AR	C
JEC	0.25	0.30	0.49
TagProp	0.23	0.29	0.50
LSR	0.37	0.45	0.67
Ours	0.39	0.48	0.72

For these baseline methods, the evaluation results reported in [9] are directly cited. Experimental results using only the SIFT BoW feature on both datasets are shown in Table 2, and results using 10 kinds of features on Flickr30Concepts are presented in Table 3.

For Core5k dataset, the proposed method outperforms previous methods by a large margin, especially for DLC and TMC, which have been analyzed in Section 1. Note that the pre-processing steps of obtaining S and T in our method correspond to the LSR method, which is far more delicate in the design of group-sparsity regularizer and soft fusion of coefficients. However, the LSR method is highly dependent on initial labels, thus, if some critical tags are removed, the sparse reconstruction may turn out inaccurate. Our method, on the other hand, seeks a balance between low-rank completion and sparse reconstruction, thus its ability to recover latent data gets preserved.

For the Flickr30Concepts dataset, the increase in performance with respect to LSR is not so significant as for Core5k dataset, since images contained in Flickr30Concepts have richer initial labels than images in the former dataset, thus the requirement for robustness towards noisy initial tags is more essential for Core5k. Note that JEC and TagProp both perform tag propagation according to the similarities defined by distances in feature space, thus all suffer from the problem which has been mentioned in Section 1.

Finally, compared with results using only SIFT BoW feature, performances using 10 types of features get substantially improved, both for the LSR method and the proposed one, which once more demonstrates the superiority of multiple features.

5. CONCLUSIONS

A novel tag completion algorithm is proposed in this paper, which is characterized by the low-rank, error sparsity, and the ability to preserve local linear reconstruction structures in the compressed low-dimensional feature space and tag space. Extensive experiments conducted on the well-known Core5k dataset and the real-world Flickr30Concepts dataset demonstrate the effectiveness and efficiency of the proposed algorithm, where our method outperforms prior methods by a large margin.

6. REFERENCES

- [1] Liang Zheng, Shengjin Wang, Ziqiong Liu, and Qi Tian, "Lp-norm idf for large scale image search," in *Computer Vision and Pattern Recognition (CVPR), IEEE Conference on. IEEE*, 2013, pp. 1626–1633.
- [2] Liang Zheng, Shengjin Wang, Wengang Zhou, and Qi Tian, "Bayes merging of multiple vocabularies for scalable image retrieval," in *Computer Vision and Pattern Recognition (CVPR), IEEE Conference on. IEEE*, 2014.
- [3] Liang Zheng, Shengjin Wang, Ziqiong Liu, and Qi Tian, "Packing and padding: Coupled multi-index for accurate image retrieval," in *Computer Vision and Pattern Recognition (CVPR), IEEE Conference on. IEEE*, 2014.
- [4] Ameesh Makadia, Vladimir Pavlovic, and Sanjiv Kumar, "A new baseline for image annotation," in *Computer Vision–ECCV*, vol. 5304, pp. 316–329. Springer, 2008.
- [5] Matthieu Guillaumin, Thomas Mensink, Jakob Verbeek, and Cordelia Schmid, "Tagprop: Discriminative metric learning in nearest neighbor models for image auto-annotation," in *Computer Vision, IEEE 12th International Conference on. IEEE*, Sept 2009, pp. 309–316.
- [6] Yin Zheng, Yu-Jin Zhang, and Hugo Larochelle, "Topic modeling of multimodal data: an autoregressive approach," in *Computer Vision and Pattern Recognition (CVPR), IEEE Conference on, 2014*.
- [7] Guangyu Zhu, Shuicheng Yan, and Yi Ma, "Image tag refinement towards low-rank, content-tag prior and error sparsity," in *Proceedings of the international conference on Multimedia*. ACM, 2010, pp. 461–470.
- [8] Lei Wu, Rong Jin, and A.K. Jain, "Tag completion for image retrieval," *Pattern Analysis and Machine Intelligence, IEEE Transactions on*, vol. 35, no. 3, pp. 716–727, 2013.
- [9] Zijia Lin, Guiguang Ding, Mingqing Hu, Jianmin Wang, and Xiaojun Ye, "Image tag completion via image-specific and tag-specific linear sparse reconstructions," in *Computer Vision and Pattern Recognition (CVPR), IEEE Conference on. IEEE*, 2013, pp. 1618–1625.
- [10] Xiaobai Liu, Shuicheng Yan, Tat-Seng Chua, and Hai Jin, "Image label completion by pursuing contextual decomposability," *ACM Transactions on Multimedia Computing, Communications, and Applications (TOMCCAP)*, vol. 8, no. 2, pp. 21, 2012.
- [11] Sihyoung Lee, Wesley De Neve, Konstantinos N Plataniotis, and Yong Man Ro, "Map-based image tag recommendation using a visual folksonomy," *Pattern Recognition Letters*, vol. 31, no. 9, pp. 976–982, 2010.
- [12] Dong Liu, Shuicheng Yan, Xian-Sheng Hua, and Hong-Jiang Zhang, "Image retagging using collaborative tag propagation," *Multimedia, IEEE Transactions on*, vol. 13, no. 4, pp. 702–712, 2011.
- [13] Dong Liu, Xian-Sheng Hua, Meng Wang, and Hong-Jiang Zhang, "Image retagging," in *Proceedings of the international conference on Multimedia*. ACM, 2010, pp. 491–500.
- [14] Miao Zheng, Jiajun Bu, Chun Chen, Can Wang, Lijun Zhang, Guang Qiu, and Deng Cai, "Graph regularized sparse coding for image representation," *Image Processing, IEEE Transactions on*, vol. 20, no. 5, pp. 1327–1336, 2011.
- [15] Bao-Di Liu, Yu-Xiong Wang, Yu-Jin Zhang, and Yin Zheng, "Discriminant sparse coding for image classification," in *Acoustics, Speech and Signal Processing (ICASSP), IEEE International Conference on. IEEE*, 2012, pp. 2193–2196.
- [16] Bao-Di Liu, Yu-Xiong Wang, Yu-Jin Zhang, and Bin Shen, "Learning dictionary on manifolds for image classification," *Pattern Recognition*, vol. 46, no. 7, pp. 1879–1890, 2013.
- [17] Bin Shen, Wei Hu, Yimin Zhang, and Yu-Jin Zhang, "Image inpainting via sparse representation," in *Acoustics, Speech and Signal Processing (ICASSP), IEEE International Conference on. IEEE*, 2009, pp. 697–700.
- [18] Bin Shen and Luo Si, "Non-negative matrix factorization clustering on multiple manifolds.," in *AAAI*, 2010.
- [19] Y Wu, B Shen, and H Ling, "Visual tracking via online non-negative matrix factorization," *Circuits and Systems for Video Technology, IEEE Transactions on*, vol. 24, no. 3, pp. 374–383, March 2014.
- [20] Honglak Lee, Alexis Battle, Rajat Raina, and Andrew Ng, "Efficient sparse coding algorithms," in *Advances in neural information processing systems*, 2006, pp. 801–808.